ГОДИШНИК НА УНИВЕРСИТЕТА ПО АРХИТЕКТУРА, СТРОИТЕЛСТВО И ГЕОДЕЗИЯ
СОФИЯ

Том 49 2016 Брой 3
Volume Issue

ANNUAL OF THE UNIVERSITY OF ARCHITECTURE, CIVIL ENGINEERING AND GEODESY
SOFIA

Приета: 18.03.2016 г.
Преработена: 11.04.2016 г.
Одобрена: 22.04.2016 г.

AN APPLICATION OF BEM-FEM HYBRID TECHNIQUE FOR SOIL-STRUCTURE INTERACTION PROBLEMS IN TIME DOMAIN THROUGH ANSYS SOFTWARE

S. Parvanova[1], G. Vasilev[2]

Keywords: *boundary element method, hybrid models, wave propagation, ANSYS*

ABSTRACT

A precise and accurate time-domain analysis is essential for the proper calculation of many sophisticated effects associated with the soil-structure interaction phenomena. The aim of the present work is to present, verify and insert in simulations a numerical procedure for correct and reliable modeling and analysis of soil-tunnel systems subjected to transient type excitations. The numerical procedure applied is a hybrid one in which the finite element method (FEM) and the boundary element method (BEM) are brought together to form the BEM-FEM hybrid model. In that model the infinite soil half-space is modeled by BEM in Laplace domain and the finite size near field zone is treated by FEM in time domain. Further, convolution quadrature method (CQM) is combined with the direct time integration scheme of Newmark to perform the final time domain solution of the whole system.

1. Introduction

The soil-structure interaction (SSI) systems are among the most commonly analysed problems in the computational mechanics and seismic wave propagation area. Despite the many recent developments of SSI problems, including high-performance models and

[1] Sonia Parvanova, Assoc. Prof. Dr. Eng., Dept. "Structural Mechanics", UACEG, 1 H. Smirnenski Blvd., Sofia 1046, e-mail: slp_fce@uacg.bg
[2] Georgi Vasilev, Chief Assist. Dr. Eng., Dept. "Structural Mechanics", UACEG, 1 H. Smirnenski Blvd., Sofia 1046, e-mail: gpekov@gmail.com

computational tools exposed in numerous scientific journals, their further improvement still attracts the attention of researchers. The seismic response of buried structures and their interaction with surrounding soil stratum with the relevant wave propagation is a complex engineering problem treated by analytical, semi-analytical, numerical or hybrid approaches. The former techniques are restricted to relatively simple geometry and continuous media which makes them of rather limited engineering use. The latter ones are widely used with the advance of the modern computational technologies, the problem is that numerical methods have merits and drawbacks, which makes them applicable for certain classes of problems and inappropriate for others. One solution to this paradox is the combined formulation which allows to profit from the advantages of different approaches avoiding their respective drawbacks. Hybrid techniques are often based on the use of two mutually complementary numerical methods.

The historical sketch of the SSI models starts with the pioneering work of Winkler [1] where the supporting soil is replaced by a bed of elastic or nonlinear springs and dashpots resting on a rigid base. Since then SSI models have been constantly improved and the available literature that traces their progress is quite voluminous. That's why in what follows, we will restrict the discussion to SSI problems which include underground structures embedded in infinite half-plane treated by hybrid techniques. Undoubtedly, nowadays the finite element method (FEM) is the most used and powerful approach in handling various classes of problems in engineering practice. At the same time boundary element method (BEM) is the most appropriate technique for modelling of infinite and semi-infinite domains. One of the first BEM-FEM couplings in elasto-statics could be found in the work of Brebbia and Dominguez [2] and later applied for various SSI problems in elasto-dynamics in Wolf [3, 4]. Here should be mentioned 3D hybrid computational schemes based on the FEM and BEM developed in Wang and Schmid [5], Manolis et al. [6], Bode et al. [7], Von Estorff and Hagen [8], Padron et al. [9], Romero et al. [10], Galvin and Romero [11], François et al. [12]. More recently a combination between the method of fundamental solutions (MFS) and FEM was developed in [13] for modelling and dynamic analysis of 2D SSI systems, and hierarchical BEM-FEM coupling was presented in [14] for 3D SSI problems, all in frequency domain. Scaled boundary finite element method (SBFEM) with FEM coupling can be found in [15], [16]. An efficient frequency dependent hybrid approach for modelling of underground structures in layered geological stratum embedded in an elastic infinite half-plane is given in [17]. A hybrid finite difference – BEM model was developed to evaluate the seismic wave field within a finite geological cross section containing an underground structure in [18].

Generally speaking, two categories of hybrid techniques could be distinguished, see Johnson [19] and Helbig [20]: (a) hybrid approaches based on a two-step procedure; (b) all-in-one, source–path–site unified computational approach. In the first group of hybrid techniques the structure and near field soil-profile are treated by one numerical method, while the laterally homogeneous far field infinite zone is analysed by other numerical technique or analytical methods. In the first step the infinite half-plane is considered excluding the heterogeneities due to the presence of a structure in the near soil-profile as well as relief peculiarities. The relative elastic wave field is computed and then used as input in the second stage where the near soil-profile with the structure is analysed as a finite region. In this two-step procedure the common interface boundaries are perfectly permeable to wave moving from the far-field half-space to the near soil zone. The main disadvantage of the hybrid two-step techniques is that in subsequent steps past the first, any interaction between the backscattering waves from the local heterogeneity with the incoming wave fields emanating from the deeper layers of the geological profile is neglected. Consequence of this impropriety is that waves excited from a source in the near soil profile (for example explosion on train) cannot be modelled. The accuracy of the results depends on the size of the near-field zone considered in the second step. The farther boundaries from the local heterogeneities the more accurate solution, respectively

the size of the near-field zone must be chosen so that scattered fields are negligibly small at its contours. Relatively less common are the second type of hybrid techniques considering and treating simultaneously the whole system: far-field semi-infinite zone, wave path, near-field region plus existing heterogeneities. The developed here hybrid technique follows in this group, where a full interaction between far-field and near-field zones is established satisfying traction equilibrium and displacement compatibility at the common interface. Contrary to the two-step procedure, where the displacement components and stress fields in the infinite half-plane are obtained in the first step, here they could be derived after the solution of the near-field zone. In this case any interaction between the waves scattered and reflected from the local heterogeneity with the incoming wave fields is taken into account. The disadvantage of all-in-one hybrid techniques is the demanding of large computational resources when the seismic source-receiver distances are too large or even inapplicability when these distances exceed tens of kilometres.

The BEM applications in elastodynamics are based on either the direct time-domain formulations or transformed domain approaches in which time dependence is removed by taking a Fourier, Laplace or other integral transform with respect to the time variable. Time domain approaches are capable of handling nonlinear behaviour in the medium or contact interfaces in case of multi-regions, while the frequency domain analysis is applicable only for linear problems. Both formulations have well known merits and drawbacks, as for example: in the classical time-domain BEM the spatial and time discretization are not independent from each other; frequency analysis requires large memory or CPU time in case of high frequencies compared to transient analysis. The latter statement is true, but could be overturned because frequency dependent solution for particular frequency is independent from the others while certain time solution depends on all previous time steps. Contemporary multi-core computers allow subdivision of frequency interval equal to the number of cores and their simultaneous calculation, while such procedure is not possible for time-interval. Besides the fact that frequency dependent fundamental solutions (FS) reduce the hyperbolic partial differential equation of motion to elliptic one, obviously easier for mathematical modelling, they don't have competitor in the areas where time-dependent FS are not available. The problem with inapplicability of the frequency dependent formulations for nonlinear problems could be overcome by the procedure proposed by Shanz and Antes [21]. They proposed BEM based on the Operational Quadrature Methods developed by Lubich [22] where the Riemman convolution integral is numerically approximated by a quadrature formula whose weights are determined by the fundamental solution in Laplace transform and this leads directly to time-dependent solutions obtained by linear multistep method. So, this procedure allows using BEM based on Laplace variable /frequency dependent fundamental solutions and at the same time solutions are directly obtained in the time-domain. Namely this procedure is applied in the current transient solution for far-field zone treated by BEM and one additional reason supporting such decision is that the authors have verified software based on frequency dependent FS [23 – 26].

To sum up, the aim of the present work is to reveal the potentials of the hybrid BEM-FEM computational technique for evaluation of dynamic behaviour and seismic response of soil-structure systems in time domain. The current analysis includes as a whole the dynamic interaction of the engineering structure itself together with the semi-infinite soil region in which the structure is placed and the dynamic excitation with the relevant wave propagation. The excitation could be natural as earthquake, technically induced like railway or vehicle traffic, or human made as explosions or foot traffic, which are all of fundamental interest in soil dynamics and civil engineering. The soil-region could be layered or homogeneous, the mechanical properties could be isotropic, anisotropic or poro-elastic, the only limitation for the far field soil zone is to have linear elastic behaviour. Since the present analysis is developed,

respectively restricted, to 2D plane problems the engineering structure must be the one that allows modelling in plane-strain state. In engineering practice such structures are tunnels and pipelines. The proposed here hybrid technique allows nonlinear behaviour of the structural components, nonlinear soil-structure contact zone or nonlinearities in the near field geological profile.

The proposed computational scheme is realized in the following steps: 1) the discrete mechanical BEM formulation of the seismically active geological environment and the seismic excitation is generated in complex (Laplace or Fourier) domain; 2) by using Lubich's Operational Quadrature approach [21, 22] the complex mechanical BEM formulation is converted in discrete transient FEM formulation to finally obtain the time-dependent stiffness matrix and load vector for the infinite far field domain; 3) the far filed infinite domain is coupled with the FEM model of the near field and the structure, and linear multi-step method is applied for determination of the transient response of the whole soil-structure system.

2. Problem formulation

The definition of the current problem has been extensively described in papers [17, 27 – 29]. More specifically a hybrid BEM-FEM approach in frequency domain has been developed in [17]. Different transformations from frequency to time domain are given in [27] where the accuracy, reliability, and convergence of the time dependent hybrid algorithms are demonstrated by comparisons of the results against different numerical models. Finally, an application of time dependent algorithm for real practical problems is demonstrated in references [28, 29]. For completeness and consistency of the current paper the problem formulation will be briefly described in this section.

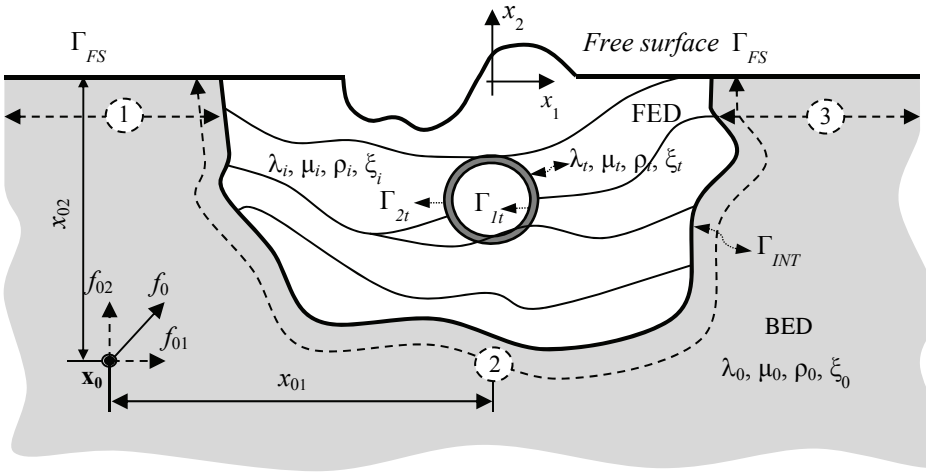

Fig. 1. Problem formulation scheme

The domain under consideration is an infinite half-plane containing underground structure layered geological profile and the excitation is transient seismic source with a prescribed magnitude $f_{0,i}$, (I = 1, 2). Plane-strain state and respectively in-plane wave motion in the plane $x_3 = 0$ of a Cartesian coordinate system $Ox_1x_2x_3$ is assumed, see Fig. 1. This half-plane is divided into two domains: (a) boundary element domain (BED) describing semi-

infinite homogeneous far-field geological region, containing flat free surface boundary Γ_{FS}; (b) finite element domain (FED) comprising N non-parallel layers representing near soil profile, free surface relief of arbitrary geometry, and finally a lined infinite cylindrical tunnel with Lame constants, density and material damping λ_t, μ_t, ρ_t, ξ_t, correspondingly. The material properties of the homogeneous far filed zone are λ_0, μ_0, ρ_0, ξ_0, while those for the *i*-th layer with interface boundary Γ_i in the FED are denoted by λ_i, μ_i, ρ_i, ξ_i, I = 1, 2, 3, …, N. Both domains are connected by contact interface denoted Γ_{INT} of arbitrary smooth shape (discontinuities are not allowed since positive unit normal must be uniquely defined along the common boundary). The concentrated at point $\mathbf{x}_0$ seismic body force is $F_i(\mathbf{x},t) = f_{0i} g(t) \delta(\mathbf{x}, \mathbf{x}_0)$, where its time function is $g(t)$ and δ is the Dirac delta function. The dynamic equilibrium equation is

$$\sigma_{ij,j}(x_1, x_2, t) = \rho \frac{\partial^2 u_i(x_1, x_2, t)}{\partial t^2} + F_i(x_1, x_2, t), \tag{1}$$

where: $\sigma_{ij} = C_{ijkl}(x_2) u_{k,l}$, $C_{ijkl}(x_2) = \lambda(x_2)\delta_{ij}\delta_{kl} + \mu(x_2)(\delta_{ik}\delta_{jl} + \delta_{il}\delta_{jk})$, δ_{ij} is Kronecker's delta symbol and comma subscripts denote partial differentiation with respect to the spatial coordinates, while the summation convention over repeated indices is implied. The well-known boundary conditions could be found in [28, 29].

3. Hybrid BEM-FEM algorithm

3.1. BEM formulation in complex (Laplace or Fourier) domain for the far field semi-infinite zone

The BEM formulation is based on the complex domain approach where time dependence is removed by taking a Fourier or Laplace transform with respect to the time variable. In this case the original hyperbolic partial differential equation of motion (1) is reduced to elliptic one along $\Gamma_{BED} = \Gamma_{FS} \cup \Gamma_{INT}$ with respect to the complex variable z:

$$\begin{aligned} c_{ij} u_j^{(BED)}(\mathbf{x}, z) = & \int_{\Gamma_{BED}} U_{ij}^{*(BED)}(\mathbf{x}, \xi, z) t_j^{(BED)}(\xi, z)\, dS(\xi) - \\ & - \int_{\Gamma_{BED}} P_{ij}^{*(BED)}(\mathbf{x}, \xi, z) u_j^{(BED)}(\xi, z)\, dS(\xi) + \\ & + f_{0i}\, g(z)\, U_{ij}^{*(BED)}(\mathbf{x}, \mathbf{x_0}, z) \end{aligned} \tag{2}$$

Here: z is the circular frequency ω or the Laplace variable s, related with the well-known relation $s = i\omega \leftrightarrow \omega = -is$, where i is the imaginary unit; $g(z)$ is the Fourier or Laplace transform of the time-history function describing the dynamic excitation; c_{ij} is the jump term depending on the local geometry at the collocation point $\mathbf{x}$; $\mathbf{x}$ and ξ are the position vectors of the source-receiver couple; $t_i = \sigma_{ij} n_j$ are the tractions and n_j are the components of the

outward normal vector; $\mathbf{U}_{ij}^{*(BED)}$ is the displacement fundamental solution of the governing equation in complex domain; $\mathbf{P}_{ij}^{*(BED)}$ is the corresponding traction.

3.2. Conversion of the BEM model of the BED into one macro-finite element (FE)

Coupling algorithm adopted here is so called FEM hosted, where the BED is converted into macro-finite element, the nodal forces are expressed through the BED nodal tractions and the entire BEM formulation is converted to FEM like approach. Initially, reduction of the degrees of freedom (DOF) of the boundary element model is performed because the contact zone between both domains is presented by common interface Γ_{INT}. For the aim of DOF condensation the BED is divided into 3 parts: 1) left flat free surface, part of the Γ_{FS} belonging to the BED; 2) common interface Γ_{INT}; 3) right flat free surface, part of the Γ_{FS}, which falls into BED, see Fig. 1. Taking into account the zero traction boundary conditions at contours 1 and 3 the system generated after discretization of boundary integral equations (2) is transformed to the following expression:

$$\mathbf{t}_{INT} = \mathbf{B}\mathbf{u}_{INT} + \mathbf{P}, \tag{3}$$

that relates traction $\mathbf{t}_{INT}$ and displacement $\mathbf{u}_{INT}$ vectors along Γ_{INT} contour. In equation (3) $\mathbf{B}$ is a square matrix of size equal to the number of degrees of freedom of the nodes belonging to the contact interface. It depends on the BEM influence system matrices $\mathbf{G}_{ij}$ and $\mathbf{H}_{ij}$ ($i, j = 1$, 2 or 3 are associated with contours 1 – 3) along the boundary $\Gamma_{BED} = \Gamma_{FS} \cup \Gamma_{INT}$ obtained after discretization of Eq. (2). The vector $\mathbf{P}$ depends on the same influence matrices plus a load vector which takes into account the last term in Eq. (2). Detailed mathematical expressions for the matrix $\mathbf{B}$ and the vector $\mathbf{P}$ can be found in [28].

The second step in macro-FE generation is conversion of the BEM system into FEM like system, respectively replacement of the interface tractions $\mathbf{t}_{INT}$ with equivalent nodal forces $\mathbf{F}_{INT}$. This relation is obtained as $\mathbf{F}_{INT} = \mathbf{M}\mathbf{t}_{INT}$, where the matrix $\mathbf{M} = \bigcup_{e} \int_{-1}^{1} \mathbf{N}^T \mathbf{N} J d\xi$ (J is the Jacobian, ξ is intrinsic coordinate), whose components are numerically derived as a product of the traction shape functions ($\mathbf{N}$) for the particular boundary element e, see [17]. Substituting Eq. (3) in this relation the following expression is obtained, which is a FEM like discrete system of equations, necessary for the formulation of the BED as a single macro-finite element:

$$\mathbf{F}_{INT} = \mathbf{K}^{(BED)}\mathbf{u}_{INT} + \mathbf{R}\,. \tag{4}$$

Here $\mathbf{K}^{(BED)} = \mathbf{M}\mathbf{B}$ is the stiffness matrix in complex domain and $\mathbf{R} = \mathbf{M}\mathbf{P}$ is the generalized load vector of nodal forces dependent on the traction load vector $\mathbf{P}$ after the condensation procedure, see [17].

3.3. Derivation of time-dependent stiffness matrix and load vector

The stiffness matrix from equation (4), for the BED model, is firstly obtained in Laplace domain. Afterwards Lubich's Convolution Quadrature (LCQ) rules [21, 22] are applied and the stiffness matrix in time domain is derived. The *k*-th time dependent stiffness matrix, at time $t_k = k\Delta t$ (Δt is the time step), is $\mathbf{K}_k(t_k) = L^{-1}\left(\hat{\mathbf{K}}(s)\right) = \boldsymbol{\omega}_k(\Delta t)/\Delta t$. Here $\hat{\mathbf{K}} = \mathbf{K}^{(BED)}$ is the stiffness matrix derived in Laplace domain, while its inverse Laplace transform $L^{-1}\left(\hat{\mathbf{K}}(s)\right)$ is expressed through the matrices $\boldsymbol{\omega}_k$ being the Lubich's convolution quadrature weights (see [21, 22]).

The nodal-force vector $\mathbf{R}$ from equation (4) is firstly obtained in frequency (Fourier) domain, then by inverse discrete fast Fourier transform the vector is derived in time domain. The *k*-th time dependent load vector, at time $t_k = k\Delta t$, is $\mathbf{R}_k\left(t_k\right) = F^{-1}\left(\mathbf{R}(\omega)\right)$.

3.4. Implementation of the macro-finite element in ANSYS software via the ANSYS user programmable features (UPFs)

The FED is modelled by 8-noded plane finite elements with 16 DOF for plane strain state (PLANE82). The BED represented by time dependent stiffness matrix and load vector is implemented in the numerical model as a single macro-FE. Both the FE and the BE time-dependent models are coupled by satisfaction of the nodal compatibility and equilibrium conditions required for all available DOF on the BED-FED contact surface. The final discrete system of equations of the coupled model in time domain, which is obtained after application of the convolution theorem, is as follows:

$$\sum_{k=1}^{j} \mathbf{K}_k \mathbf{u}_{j-k+1} = -\mathbf{R}_j, \quad j = 1, ..., N, \tag{5}$$

where N is the total number of time steps. The real dynamic stiffness matrices are $\mathbf{K}_k = \mathbf{K}_k^{(BED)} + \mathbf{K}_k^{(FED)}$, where the subscript designates the discrete time value ($t_k = k\Delta t$) at which the quantities are calculated. In this system the only unknowns are the components of the displacement vector $\mathbf{u}_j$ at time t_j, since all the displacement components in the previous time steps, included in the discrete sum, are previously calculated. This dependence on the previous time steps and not on the future ones is consequence of the causality of the system. The stiffness matrices $\mathbf{K}_k^{(BED)}$ and load vectors $\mathbf{R}_j$ are generated with the authors' code developed in MATLAB, while $\mathbf{K}_k^{(FED)}$ is generated by the ANSYS software.

One of the major differences between BEM and FEM, which must be pointed here, is that the latter method leads to sparse symmetric positive definite matrices, while the former one, based on a collocation technique, leads to full non-symmetric matrices. Specifically for our approach, when full method of solution in transient FEM analysis is chosen and ANSYS detects the presence of structure with unsymmetrical and fully populated matrices it automatically switches to a solver for dealing with the arisen unsymmetrical system of equations.

4. Numerical results

The results obtained by the hybrid BEM-FEM algorithm in time domain have been compared against solutions derived via the conventional BEM authors' software in references [27 – 29]. The accuracy of the BEM authors' code is demonstrated in [24, 26] where the P- and SV-scattered displacement and stress fields, by a semi-circular canyon or semi-elliptic hill, sub-surface cavity or alluvial basin, are compared with numerical and analytical solutions of other authors. The conventional BEM solution in time domain is obtained by inverse discrete fast Fourier transform of the original results. Although the accuracy of the hybrid technique has been checked and reported for various problems, we note that detailed verification study is necessary for every particular solution in order to adjust the parameters of the numerical models in complex domain. The time dependent BEM system matrices obtained by LCQ rules from the solution in Laplace domain are sensitive not only to the BEM mesh but also to the excitation applied. The final Nyquist frequency used in complex domain modelling, which leads to the acceptable difference of the hybrid approach results with respect to the conventional BEM solution, depends on the time-history excitation function. That is why the subject of the following section prior to numerical simulations is again verification of the hybrid solution, since the parameters of the time-history function applied here are not used before.

4.1. Verification of the results obtained by hybrid technique

The numerical example, subject of the current section, is directly related to the considered in the next simulation study relatively complex soil-structure system. The verification model is a semi-circular canyon of radius a = 7 m located in an elastic, isotropic and homogeneous half-plane with material parameters: Poisson's ratio $\nu_0 = 1/3$; shear modulus $\mu_0 = 7.10^5$ kN/m^2; density $\rho_0 = 2$ t/m^3; and hysteretic damping ratio $\xi_0 = 0\%$. For verification purposes the half-plane is divided into finite (FED) and infinite (BED) domains by fictitious semi-circular interface of radius r = 10a, shown as dashed line in Fig. 2. The excitation is an embedded line source of magnitude $f_{0i} = \left(0, -1.10^6 \text{kN}\right)$ located first at point $\mathbf{x}_0 = \left(0, -150\right)$ below the flat surface, which falls within the infinite half-plane, then at point $\mathbf{x}_0 = \left(50, -21\right)$ which falls in FED. The transient concentrated force $F_i\left(\mathbf{x}, t\right) = f_{0i} g\left(t\right) \delta\left(\mathbf{x}, \mathbf{x}_0\right)$ in the source is defined by time-history function $g\left(t\right) = e^{-\alpha t} \sin(\omega_0 t)$, which has continuous Fourier transform $S(\omega) = \omega_0 / \left(\omega_0{}^2 + (\alpha + i\omega)^2\right)$. The parameters of the function are $\omega_0 = 20$ rad/s and $\alpha = 1$.

The reference model is a semi-circular canyon in a half-plane, modelled by authors' software based on conventional BEM and frequency dependent full space fundamental solutions. The BE mesh used for discretization of the free surface comprises 144 quadratic boundary elements, 48 of which located along the canyon contour. The length of the discretized flat free surface is 280 meters or 40a, measured left and right to the canyon centre. The Nyquist frequency is 30 Hz and the frequency range is divided into 400 equal steps.

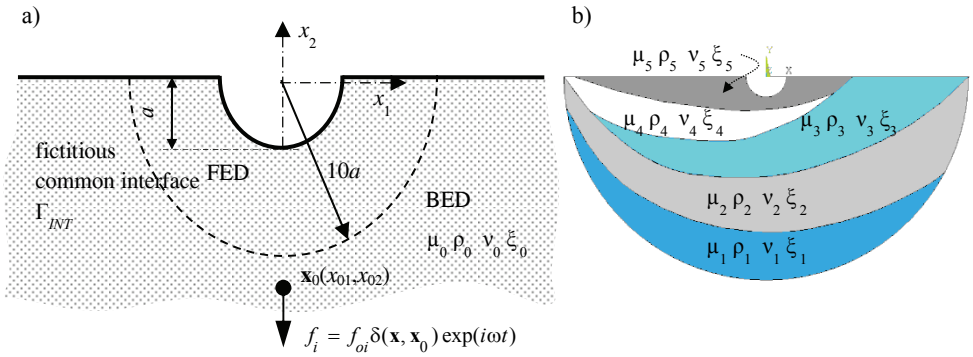

Fig. 2. Verification example: a) Geometry; b) Finite element domain

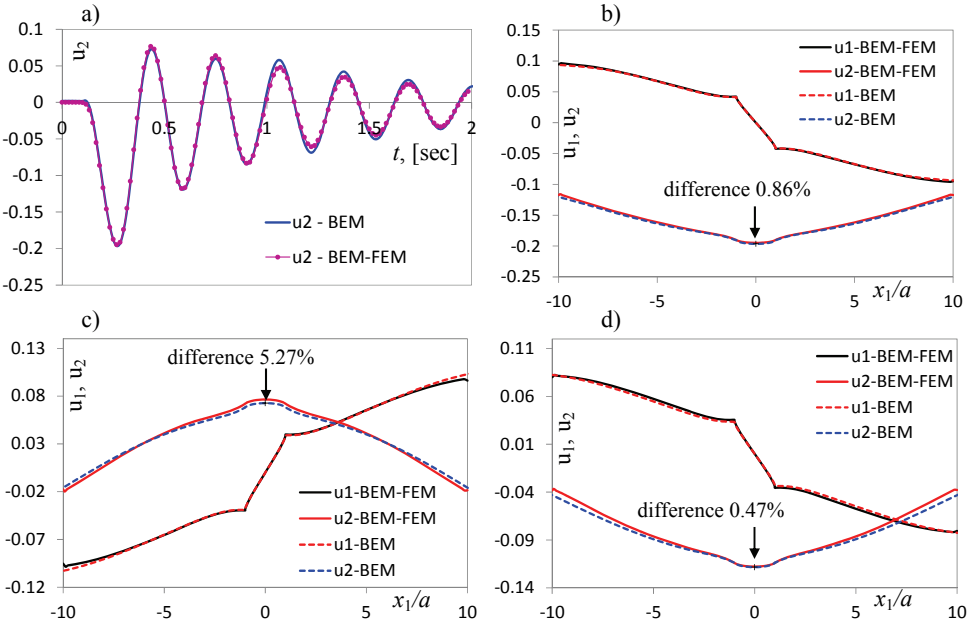

Fig. 3. Surface displacements in meters for line source located at point x_0 = (0,-150): a) Vertical displacements at bottom of the canyon versus time; Displacement components along the free surface for fixed time: b) t = 0.267 sec; c) t = 0.433 sec; d) t = 0.583 sec

The hybrid BEM-FEM model comprises two domains: infinite homogeneous half plane (BED) and multi-layered FED as shown in Fig. 2a, b. The same layer outlines are used in the following simulation study; here, for validation purposes, all layers have material properties identical with those of the half-plane. Firstly, the infinite half-plane is modelled by BEM in complex (Laplace) domain then the convolution quadrature rule is applied and time-dependent stiffness matrix for macro-FE formulation is obtained. We note that the Laplace variables are obtained based on Nyquist frequency 30 Hz in order to achieve the accuracy reported in the current study. The FE model comprises of 4618 quadratic FE (ANSYS code PLANE 82) and

one macro-finite element (MATRIX 50) with 97 nodes, generated as BED and MATLAB software code. Transient analysis is performed to the FE model, where Lubich's Convolution Quadrature algorithm is used along with Newmark's integration scheme. The unknown displacement components of the whole BEM-FEM numerical model are derived directly in time domain.

Comparisons of the results, obtained by both BEM and hybrid BEM-FEM approaches, for the deep seismic source located at point x_0 = (0,-150), are presented in Fig. 3a – d. More specifically Fig. 3a depicts vertical displacement components for bottom of the canyon (x_0 = (0,-7) versus time variable. The plots in Figs. 3b – d are free field displacement components for fixed time t = 0.2667, 0.4333 and 0.5833 sec, which corresponds to the first three extreme values of the previous graphic. The percentage differences between both solutions are marked for vertical displacements at bottom of the canyon in the corresponding free surface plots.

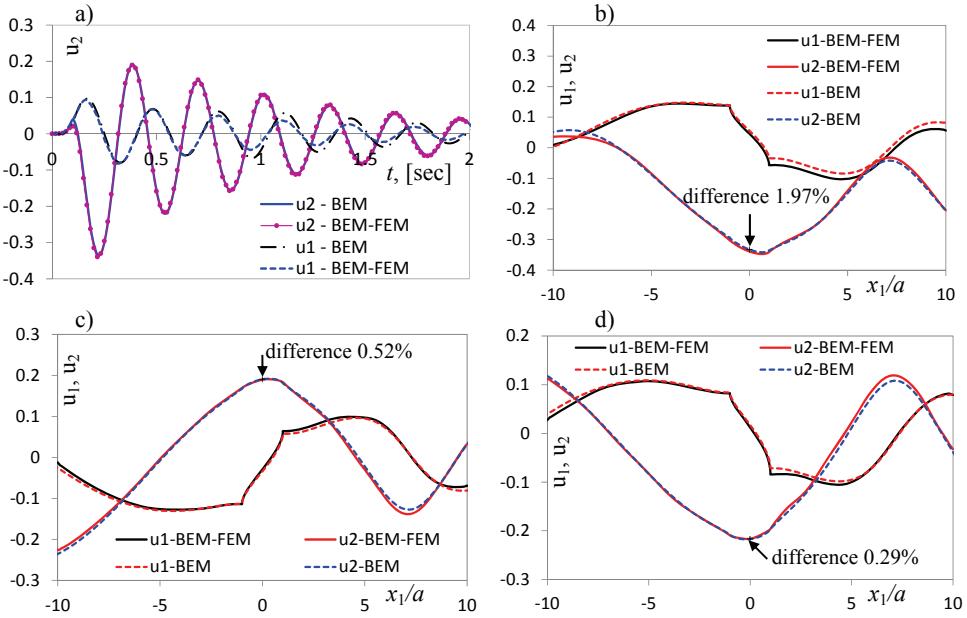

Fig. 4. Surface displacements in meters for line source located at point x_0 = (50,-21): a) Vertical displacements at bottom of the canyon versus time; Displacement components along the free surface for fixed time: b) t = 0.217 sec; c) t = 0.383 sec; d) t = 0.55 sec

The same sets for comparison are plotted in Fig. 4 but for shallow seismic source located at point x_0 = (50,-21), which falls in FED. Here the horizontal displacement at bottom of the canyon is nonzero and is also plotted in Fig. 4a. Here the time values corresponding to the first three extreme values in the vertical displacements are t = 0.2167, 0.3833 and 0.55 sec. The percentage differences between both models for vertical displacements at bottom of the canyon are marked again at the corresponding site-effect-plots. Such discrepancies cannot be totally avoided, but they are obtained for the most stringent verification test, namely the absence of any material damping. We expect that the introduction of material damping in the soil will reduce the percentage differences. Nevertheless, all presented results demonstrate satisfactorily numerical accuracy (less than or around 5%) between the present hybrid methodology and the results obtained by the conventional direct BEM formulation.

4.2. Numerical simulations

In this section we present important numerical simulations that are closely related to the engineering practice. The first model considered is the tunnel structure entirely embedded in nonhomogeneous soil-strata as shown in Fig. 5. The aim of this example is to reveal some of the important features in the tunnel engineering practice like: 1) influence of the surface relief, e.g. hills and valleys; 2) influence of the soil layering; 3) stress concentration on the tunnel contour; 4) influence of the infinite half-space and the assumed seismic wave pattern in it. Here the tunnel structure is modelled as double deck system in which we have metro lines on the lower level and two highway lanes in the upper deck, as shown in Fig. 5a. The inner radius of the structure cross section is a = 7 m, the wall thickness is 0.4 m and all other dimensions are given in Fig. 5a. The depth of burial is $h = 4a$ =28 m measured from the flat free surface. The material properties of the structure are: Young's modulus $E_t = 30000$ MPa, Poisson's ratio $\nu_t = 0.2$, material density $\rho_t = 2.5$ t/m^3 and damping coefficient $\xi_t = 0\%$. This structure is embedded in nonhomogeneous multi-layered near field zone shown in Fig. 5b. This finite region consists of five soil layers with material properties as follows: μ_1= 620 MPa, ν_1 = 1/3, ρ_1 = 1.8 t/m^3; μ_2 =500 MPa, ν_2 = 0.4, ρ_2 = 1.75 t/m^3; μ_3 = 200 MPa, ν_3 = 0.45, ρ_3 = 1.8 t/m^3; μ_4 = 70 MPa, ν_4 = 0.46, ρ_4 = 1.85 t/m^3; μ_5 = 10 MPa, ν_5 = 0.48, ρ_5 = 1.9 t/m^3. The material properties of all the layers are considered to be purely elastic, i.e. the damping coefficients are $\xi_1 = \xi_2 = \xi_3 = \xi_4 = \xi_5 = 0\%$. The upper boundary of the near field region is the traction free surface which is entirely flat or with a relief peculiarity in the middle (above the tunnel) expressed as hill/valley of height/depth h = 14 m and half-width b = 30 m. The near field lower boundary represents the near to far field contact surface Γ_{INT} chosen here to be with the shape of semicircle of radius $r = 10a$ = 70 m. In the case of a relief (not flat) the hill/valley lining is given with the spatial coordinate function $x_2(x_1) = \pm h\cos^2\left(\pi x_1 / 2b\right)$, where the plus and minus sign designates hill or valley respectively.

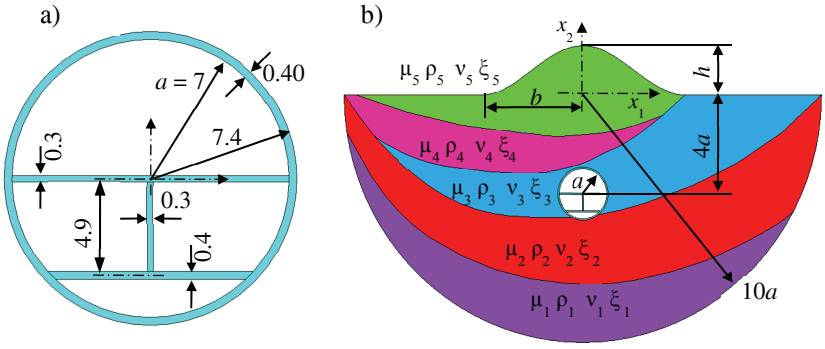

Fig. 5. Soil-Tunnel system: a) tunnel construction; b) geological strata

The nonhomogeneous soil strata are embedded in homogeneous and elastic half-plane with the following material properties: μ_0 = 700 MPa, ν_0 = 1/3, ρ_0 = 2 t/m^3 and material damping $\xi_0 = 0\%$.

The excitation to the system is seismic waves propagating in the plane of the model. This waves are considered to emanate from a line seismic source with magnitude $f_{0i} = \left(0, -1.10^6 \text{kN}\right)$, situated in the line $\mathbf{x}_0 = (0, -150)$ for far field excitation (deep source)

or the line $\mathbf{x}_0 = (50, -21)$ for near field excitation (shallow source). The temporal and spatial variation of the excitation is described with the function $F_i(\mathbf{x},t) = f_{0i}g(t)\delta(\mathbf{x},\mathbf{x}_0)$, where $g(t) = e^{-\alpha t}\sin(\omega_0 t)$ with $\omega_0 = 20$ rad/s and $\alpha = 1$.

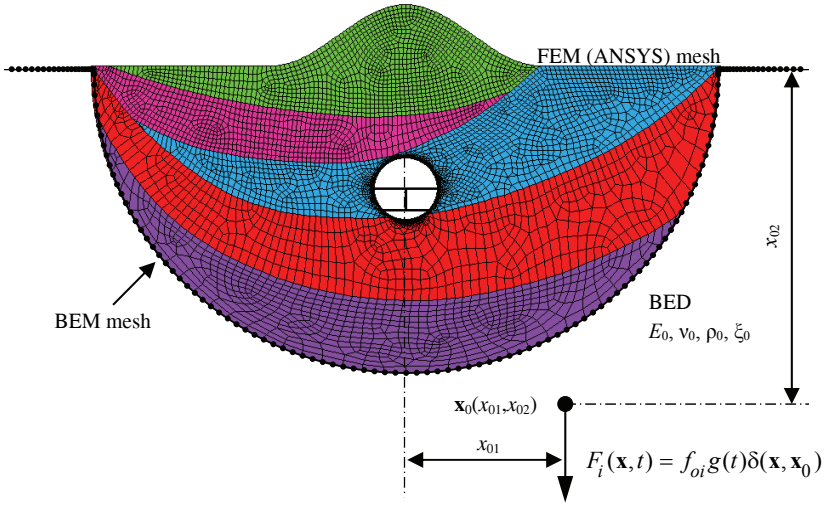

Fig. 6. Discretization of the hybrid BEM-FEM model

The boundary element model for the far-field region (the macro element) consists of 144 quadratic boundary elements, 48 of which comprise the contact surface Γ_{INT}. The length of discretization of the flat free surface is 2800 meters or 400a (40 times the radius of Γ_{INT}) left and right of the contact boundary, refer to Fig. 6. The Nyquist frequency is 30 Hz, leading to a time step size of $\Delta t = 1/60$ sec.

The finite element mesh that represents the numerical model of the finite element domain with flat/hill/valley surface consists of 8005/8731/7511 quadratic finite elements (ANSYS PLANE82) and one macro-finite element (ANSYS MATRIX50) of 97 nodes. Both meshes for the far-field region and for the near-field region are depicted in Fig. 6.

The aim of this simulation example is to reveal the influence of the surface relief to the dynamic behavior of the whole soil-tunnel system. More specifically the given plots depict the differences in the wave propagation pattern at the surface of the system.

Here, additional verification has been developed by comparing two different numerical models: 1) The soil-tunnel system is modelled with hybrid BEM-FEM technique, as proposed in this paper and 2) The entire system is modeled with FEM in the numerical environment of ANSYS. In the latter FEM model the far field zone has been elongated to a large distances from the source location, the free surface and the tunnel construction in order to prevent back-reflection of the waves on the artificial boundaries. For that purpose the semi-infinite far field domain is modeled as a semicircular area with radius of 2250 m which is equal to $15d_{deep}$, where d_{deep} = 150 m is the depth of the deep source. We note that in this FEM model we do not have solutions in Fourier or Laplace domain followed by transformations for macro FE formulation. Here only transient analysis has been performed and the seismic source is modeled as concentrated force in the node of the model, which additionally verifies the hybrid algorithm. The finite element mesh in the extended FEM model comprises of

19503/18306/18806 quadratic finite elements (ANSYS PLANE82), respectively for flat/hill/valley surface relief. This means models whose meshes are 2 – 2.5 times larger than those used in the hybrid models.

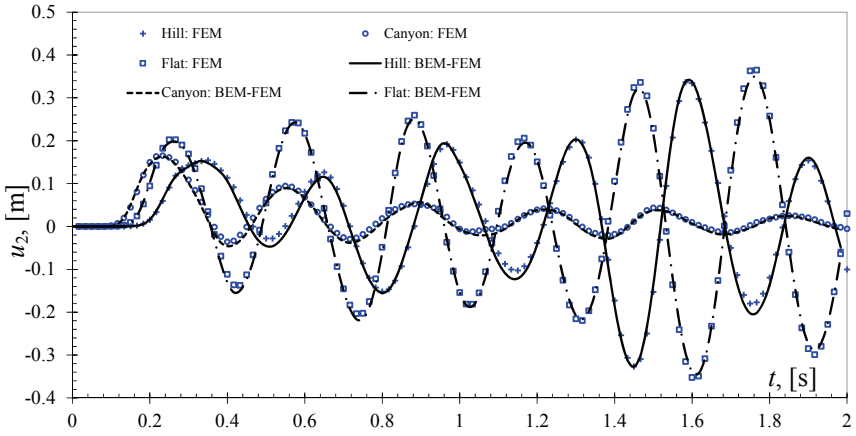

Fig. 7. Vertical displacements at top of the hill, bottom of the canyon, and x = (0,0) for the flat surface versus time for the deep source

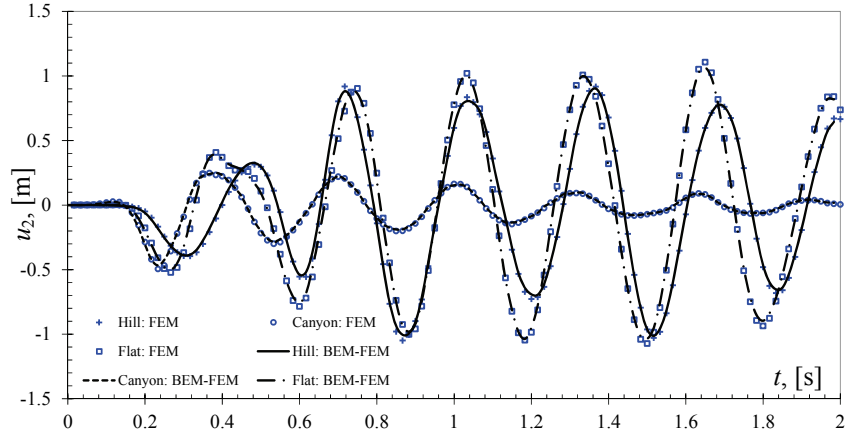

Fig. 8. Vertical displacements at top of the hill, bottom of the canyon, and x = (0,0) for the flat surface versus time for the shallow source

Comparison of the vertical displacement components at top of the hill $\boldsymbol{x}$ = (0,14), bottom of the canyon $\boldsymbol{x}$ = (0,-14), and the middle for the flat surface $\boldsymbol{x}$ = (0,0) versus time is presented in Figs. 7 and 8, for the deep $\boldsymbol{x}$ = (0,-150) and shallow $\boldsymbol{x}$ = (50,-21) sources respectively. As expected better coincidence between hybrid and pure FEM models is observed in case of the shallow source (Fig. 8), since the influence of the backscattering waves from the artificial external boundary is minimized. In order to achieve better accuracy in case of the deep seismic source (see Fig. 7) the size of the far-field zone should be extended although the observed plotting accuracy is satisfactorily.

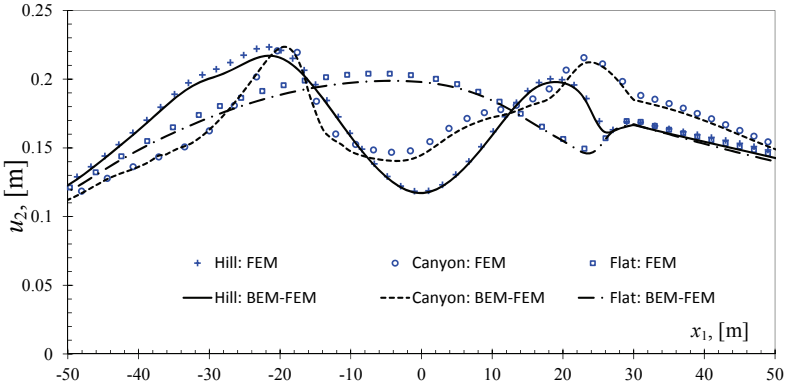

Fig. 9. Vertical displacement components at the free surface for t = 0.2667 s in case of deep source

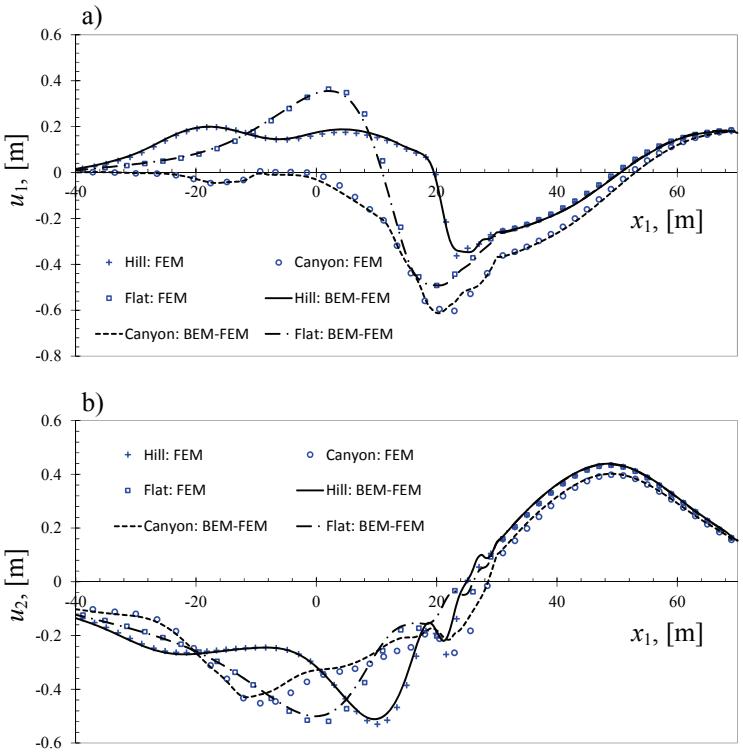

Fig. 10. Displacement components at the free surface for t = 0.2667 s in case of shallow source: a) horizontal displacements; b) vertical displacements

Similar sets of comparison for the site effects at the free surface are illustrated in Figs. 9 and 10 for the deep and shallow sources respectively. The plots are for time t = 0.2667 s which corresponds to the first peaks observed in the graphics from Figs. 7 and 8.

Figures 11 and 12 show the vertical displacement components for a point of the free surface with coordinates (-40,0) for the cases of deep and shallow seismic sources respectively. Since the point is relatively far away from the relief peculiarities, at the beginning all curves are similar and the influence of the surface inhomogeneity is missing. Comparing figures 7&8 with 11&12 we observe that in the former plots the incoming waves reach first bottom of the canyon followed by flat free surface and finally top of the hill, while in the latter plots incoming waves reach the point at the same time. Then shifting of all plots is watched since the influence of scattered and reflected waves takes place. Comparing results for center points of the relief peculiarities (Figs. 7&8) it seems that considerable deamplification is observed at bottom of the canyon while amplitudes of the displacements in case of flat free surface and hill are commensurable. Contrary, for points of the free surface, out of the peculiarities, the largest amplification is observed in case of canyon for the deep source and in the case of hill for the shallow source.

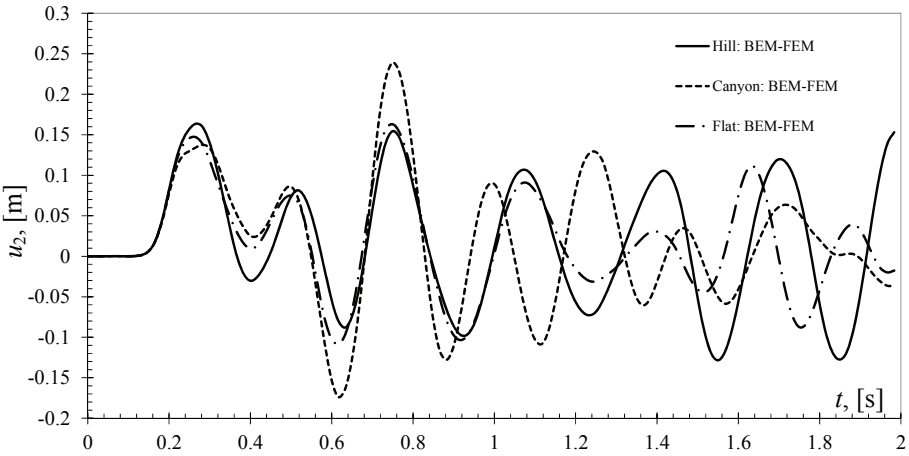

Fig. 11. Vertical displacement at x = (-40,0) versus time for the deep source

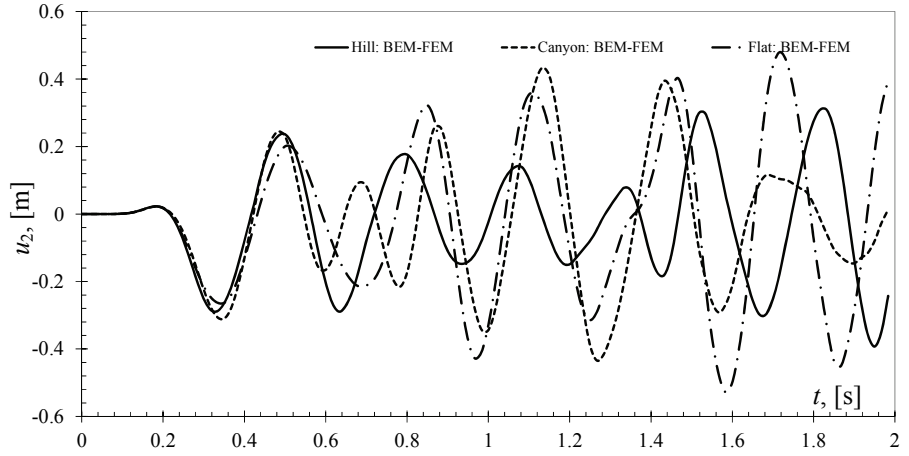

Fig. 12. Vertical displacement at x = (-40,0) versus time for the shallow source

The last set of results concerns stresses at the soil-tunnel interface from the tunnel side. Figure 13a depicts the hoop stress distribution, for fixed time t = 0.2667 s, versus the polar angle for the deep seismic source, for the three cases of surface relief: flat free surface, hill and canyon. Similar plots for the case of shallow source are shown in Fig. 13b. As expected, in the latter case stresses are considerably larger compared to the former stress distribution, due to the nearness of the source. In both cases decrease in hoop stresses is observed for the canyon peculiarity, while for the flat free surface and hill values are commensurable.

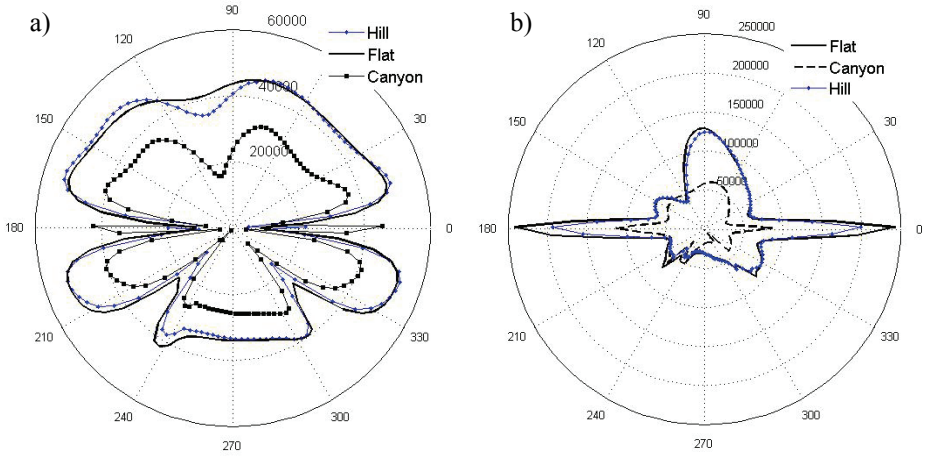

Fig. 13. Polar distribution of the hoop stresses in [kN/m^2] at t = 0.2667 s in the case of: a) deep source; b) shallow source

5. Conclusions

A hybrid BEM-FEM numerical algorithm in time domain has been presented in the current paper for 2D in-plane problems associated with the seismic response of buried tunnels in a layered half-plane containing a line transient seismic source. The numerical model of the far field soil region is modeled by BEM ising the full space elastodynamic fundamental solutions in complex domain (Laplace and Fourier) followed by transformation based on Lubich Operational Quadrature in order to obtain time-dependent stiffness matrix and load vector of the seismically active infinite half-plane. The structure, along with the surrounding near field soil-profile, is treated by FEM and ANSYS software package. In this procedure both domains work together and the full interaction between incident and scattered waves is taken into account.

The numerical algorithm proposed here could be easily extended further for treating of both geometrical and material type of nonlinearities. At first nonlinear contact soil-tunnel could be established in order to precisely capture the stresses along the tunnel interface, then different nonlinear processes associated with near soil behavior could be involved in the models developed here.

6. Acknowledgements

The authors wish to acknowledge the support provided by RC&DC of UACEG-Sofia through the Grant No. BN 174/15.

LITERATURE

1. *Winkler, E.* Die Lehre von der Elasticitaet und Festigkeit, H. Dominicus, Prag, 1867.
2. *Brebbia, C. A., J. Dominguez*. Boundary Elements: An Introductory Course, WIT Press, 1992.
3. *Wolf, J. P.* Dynamic Soil Structure Interaction, New Jersey: Prentice-Hall, Inc., Englewood Cliffs, 1985.
4. *Wolf, J. P.* Soil Structure Interaction Analysis in Time Domain, New Jersey: Prentice-Hall, Inc., Englewood Cliffs, 1988.
5. *Wang, S., G. Schmid*. Dynamic structure–soil–structure interaction by FEM and BEM. Computational Mechanics **9**, 347–57, 1992.
6. *Manolis, G. D., P. I. Tetepoulidis, D. G. Talaslidis, G. Apostofidis*. Seismic analysis of buried pipeline in a 3D soil continuum, Engineering Analysis with Boundary Elements **15**, 371–394, 1995.
7. *Bode, Ch., R. Hirschauer, S. Savidis*. Soil-structure interaction in the time-domain using Half-space Green's functions, Soils Dynamics and Earthquake Engineering **22**, 283–295, 2002.
8. *Von Estorff, O., Ch. Hagen*. Iterative coupling of FEM and BEM in 3D transient elastodynamics, Engineering Analysis with Boundary Elements **29**, 775–787, 2005.
9. *Padron, L. A., J. J. Aznarez, O. Maeso.* Dynamic structure–soil–structure interaction between nearby piled buildings under seismic excitation by BEM-FEM model, Soil dynamics and earthquake engineering **9**(6), 1084–96, 2009.
10. *Romero, A., P. Galvín, J. Domínguez*. 3D non-linear time domain FEM–BEM approach to soil–structure interaction problems, EABE **37**(3), 501–512, 2013.
11. *Galvin, P., A. Romero*. MATLAB toolbox for soil–structure interaction analysis with finite and boundary elements, Soil Dynamics and Earthquake Engineering **57**, 10–14, 2014.
12. *Françoi,s S., P. Coulier, G. Degrande*. Finite element–boundary element coupling algorithms for transient elastodynamics, Engineering Analysis with Boundary Elements **55**, 104–121, 2015.
13. *L. Godinho, P. Amado-Mendes, A. Pereira, D. Jr. Soares.* A coupled MFS-FEM model for 2-D dynamic soil-structure interaction in the frequency domain, Computers and Structures **129**, 74–85, 2013.
14. *P. Coulier, S. François, G. Lombaert, G. Degrande.* Coupled finite element–hierarchical boundary element methods for dynamic soil–structure interaction in the frequency domain, International Journal of Numerical Methods in Engineering. **97**, 505–530, 2014.

15. *Wolf, J. P.* The Scaled Boundary Finite Element Method, John Wiley & Sons Ltd, England, 2003.

16. *Wolf, J. P., C. Song*. The scaled boundary finite-element method – a primer: derivations, Computers & Structure **78**, 191–201, 2000.

17. *Vasilev, G., S. Parvanova, P. Dineva, F. Wuttke*. Soil-structure interaction using BEM-FEM coupling through ANSYS software package, Soil Dynamics and Earthquake Engineering 70 (2015), 104–117, DOI:10.1016/j.soildyn.2014.12.007, 2014.

18. *Manolis G., S. Parvanova, K. Makra, P. Dineva.* Seismic response of buried metro tunnels by a hybrid FDM-BEM approach, Bulletin of Earthquake Engineering, DOI: 10.1007/s10518-014-9698-6, 2015.

19. *Johnson, J. J. (ed)*. Soil–structure-interaction: the status of current analysis methods and research, research report NUREG CR-1780, Nuclear Regulatory Commission, Washington, 1981.

20. *Helbig, K. (ed)*. Modelling the earth for oil exploration, Pergamon Press, London, 1994.

21. *Schanz, M., H. Antes*. A new visco- and elastodynamic time domain boundary element formulation, Comp. Mech. **20**(5), 452–459, 1997.

22. *Lubich, C.* Convolution quadrature and discretized operational calculus -I. Numerische Mathematic **52**(2), 129–145, 1988.

23. *Parvanova, S., P. Dineva, G. Manolis, F. Wuttke*. Diffraction of In-Plane (P, SV) and Anti-Plane (SH) Waves in a Half-Space with Cylindrical Tunnels, Proceedings of International Conference on Boundary Element Techniques XIV 16-18 July 2013, Paris, France, Edited by A. Sellier, M. H. Aliabadi, ISBN: 978-0-9576731-0-6, Published by EC Ltd, UK, pp. 335–340, 2013.

24. *Parvanova, S., P. Dineva, G. Manolis.* Elastic wave fields in a half-plane with free Surface relief, tunnels and multiple buried inclusions. Acta Mechanica **225**(7), 1843–1865, 2014.

25. *Dineva, P., S. Parvanova, G. Vasilev, F. Wuttke.* Seismic Soil-Tunnels Interaction via BEM. I. Mechanical model – (PART I). Journal of Theoretical and Applied Mechanics **44**(3), 31–48, 2014.

26. *Dineva, P., S. Parvanova, G. Vasilev, F. Wuttke.* Seismic Soil-Tunnels Interaction via BEM. II. Numerical results – (PART II). Journal of theoretical and applied mechanics, **44**(4), 29–50, 2014.

27. *Parvanova, S., G. Vasilev.* Hybrid BEM-FEM algorithm for numerical modelling and analysis of 2D soil-structure systems in frequency and time domain, Annual of UACEG, Sofia, Vol. XLVIII, fascicule VIII-A, pp. 185–211, 2015 (in Bulgarian).

28. *Vasilev, G., S. Parvanova.* Hybrid BEM-FEM Algorithm in Time-Domain for Numerical Modelling of Soil-Tunnel Interaction, Proceedings of International Conference on Boundary Element and Meshless Techniques XVI 6–8 July 2015, Valencia, Spain, Edited by V. Mantic, A. Saez, M. H. Aliabadi, ISBN: 978-0-9576731-2-0, Published by EC Ltd, UK, pp. 30–37, 2015.

29. *Parvanova, S., G. Vasilev, P. Dineva and F. Wuttke*. BEM-FEM coupling in time-domain for soil-tunnel interaction, In: Sextos, A. & Manolis, G. D. (eds.). "Dynamic Response of Infrastructure to Environmentally Induced Loads" Springer International Publishing AG, Cham, Switzerland, submitted 2015.

ЕДНО ПРИЛОЖЕНИЕ НА МГЕ–МКЕ ХИБРИДЕН АЛГОРИТЪМ ЗА ЗАДАЧИ ОТ ВЗАИМОДЕЙСТВИЕ ПОЧВА–КОНСТРУКЦИЯ ВЪВ ВРЕМЕВАТА ОБЛАСТ ЧРЕЗ ANSYS

С. Първанова[1], Г. Василев[2]

Ключови думи: *метод на граничните елементи, хибридни модели, разпространение на вълни, ANSYS*

РЕЗЮМЕ

Точният и прецизен динамичен анализ във времето е от съществено значение за коректното изчисляване на множество сложни ефекти, свързани с явления от областта на взаимодействие почва–конструкция. Целта на настоящата работа е да разработи, провери и приложи в числени симулации алгоритъм за точното и надеждно моделиране и анализ на задачи от областта почва–конструкция, подложени на променливи във времето въздействия. Хибридната техника е реализирана чрез метода на граничните елементи (МГЕ) и метода на крайните елементи (МКЕ). С първия числен метод е моделирано безкрайното почвено полу-пространство в област на Лаплас, а крайната област около конструкцията е моделирана във времеви интервал чрез МКЕ и ANSYS. Впоследствие методът на операционните квадратури е комбиниран с дирекно интегриране във времето по метода на Newmark, за да се получи окнчателното решение на цялата система.

[1] Соня Първанова, доц. д-р инж., кат. „Строителна механика“, УАСГ, бул. „Хр. Смирненски“ № 1, 1046 София, e-mail: slp_fce@uacg.bg

[2] Георги Василев, гл. ас. д-р инж., кат. „Строителна механика“, УАСГ, бул. „Хр. Смирненски“ № 1, 1046 София, e-mail: gpekov@gmail.com